CHAPTER III

Selective N-Terminal Modification of Calcineurin and Calmodulin

ABSTRACT

The NMT-mediated protein labeling system described in Chapter II serves as the foundation of the work described in this chapter. We applied the principles and techniques developed for our GFP-based model system to achieve selective N-terminal labeling of two neuronal proteins, calcineurin (CaN) and calmodulin (CaM). Both proteins are implicated in the complex pathways governing learning and memory, and both have been studied by neuroscience researchers for decades. In the projects described herein, our objective was to utilize NMT and 12-ADA to site-specifically functionalize CaN and CaM for subsequent surface immobilization. (Note that surface immobilization experiments are described in Chapter IV.) We also aimed to create protein constructs that retained wild-type levels of activity even after undergoing engineering and labeling.

Because CaN is a natural substrate of NMT, we proceeded directly to expression and labeling experiments. However, CaM is not naturally myristoylated. Thus, we prepared a family of engineered CaM constructs, each displaying an NMT recognition sequence. CaN and the CaM constructs were co-expressed with NMT in the presence of 12-ADA for N-terminal labeling and purified for intact LC-MS analysis and activity assays. We were pleased to find that CaN and one of the engineered CaM constructs did retain wild-type activity, even after labeling with 12-ADA. We also confirmed, via treatment of lysate samples with an azide-reactive dye, that NMT is selective toward CaN and the engineered CaM constructs in bacteria. In summary, we extended our NMT-based protein labeling system from a model protein, GFP, to proteins that perform important functions in complex organisms.

INTRODUCTION

Calcineurin and Calmodulin

Calcineurin (CaN) is a 79-kDa heterodimeric serine/threonine phosphatase that is enriched in the brain.[1] The 60-kDa A subunit of CaN contains the catalytic domain of the enzyme as well as four other domains: a regulatory domain, an autoinhibitory domain, and domains for binding the CaN B subunit and calmodulin (CaM). Of interest for our work, the 19-kDa B subunit is naturally myristoylated.[2] It is apparent from the crystal structure of CaN (Figure III-1A) that the N-terminus of the CaN B subunit is accessible, a common feature of NMT substrate proteins.

CaN performs important functions in different systems of the body. It is involved in the signal transduction pathways of numerous cell types, including lymphocytes and kidney cells.[3] In the brain, CaN plays a role in synaptic plasticity; CaN knock-out mice experience memory deficits and exhibit characteristics related to schizophrenia, such as impaired social interaction and disrupted nesting behaviors.[4] Because CaN is highly conserved among eukaryotes and is involved in a variety of cellular processes, it has been studied extensively by neuroscientists and behavioral scientists as well as immunologists. Notably, CaN becomes active only upon binding of its A subunit by CaM.

In contrast with CaN, CaM is a small, 16-kDa, monomeric protein.[5] But, like CaN, CaM undergoes conformational changes upon binding Ca^{2+} ions. In fact, CaM is generally inactive toward the more than 100 proteins it regulates until it binds four Ca^{2+} ions (Figure III-1B), at which point it is able to activate other proteins and enzymes, including CaN. CaM is also highly conserved across eukaryotes and is present in all eukaryotic cells; it is enriched in the brain and involved in synaptic plasticity, like CaN.[6]

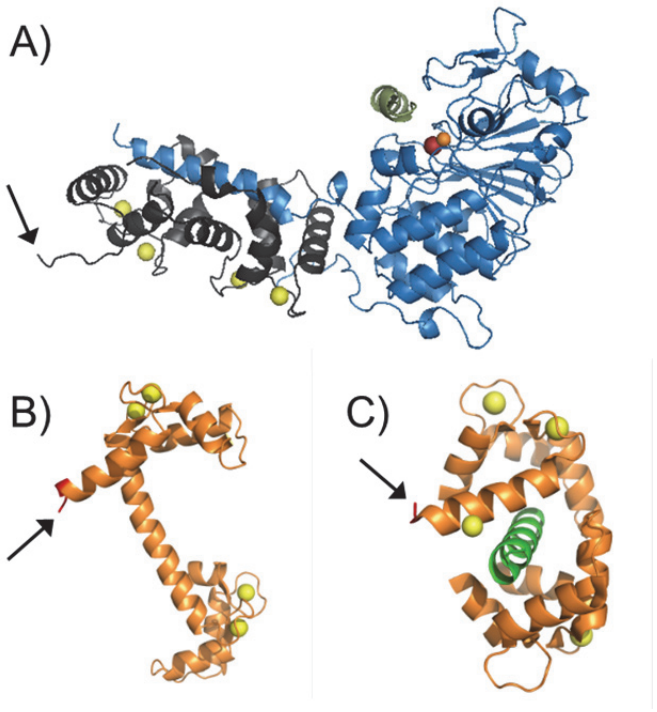

Figure III-1. Crystal structures of CaN (A) and CaM (B, C). Black arrows point to each protein N-terminus. The conformation of CaM shown in (B) is observed upon binding of four Ca^{2+} ions, and that depicted in (C) corresponds to further structural changes upon binding of a partner protein by CaM. For (A): PDB ID = 1AUI, yellow = Ca^{2+}; red = Fe^{3+}; orange = Zn^{2+}; blue = CaN A subunit; grey = CaN B subunit; green = peptide substrate. For (B): PDB ID = 1CLL and (C): PDB ID = 1CDM, yellow = Ca^{2+}; green = peptide derived from CaM kinase II, a CaM binding partner.

We were intrigued by the similarities and differences apparent upon comparison of CaN and CaM. As our interests include expanding the scope of our original NMT-mediated protein labeling system, we were particularly excited by the parallel study of a large natural NMT substrate requiring no engineering, and a small, streamlined protein that could be challenging to engineer without an accompanying loss of function. With the ultimate objective of site-specifically functionalizing both CaN and CaM to prepare

protein microarrays for high-throughput biochemical studies, we began by preparing CaM constructs that would be recognized by NMT.

Engineering CaM for NMT-Mediated Protein Labeling

In designing new CaM-based constructs for labeling with NMT, we drew inspiration from the model system described in Chapter II, in which we prepared two GFP-based constructs: yARF-GFP and Fyn-GFP. For preparation of CaM constructs, we initially worked only with the yARF recognition sequence (MGLFASK) because the Fyn recognition sequence (MGCVQCKTK) contains two cysteine (Cys, C) residues. CaM contains no Cys residues in its native form, and we hypothesized that addition of the nucleophilic thiol side chain of Cys could unfavorably alter the structure of CaM.

The first construct we prepared was yARF-6xHis-CaM (Table III-1), engineered to display the 6xHis affinity purification tag as well as the yARF sequence. Although expression, purification, and mass spectrometry experiments with this protein yielded good results, it was found to be four times less active than wild-type (WT) CaM. It was not apparent whether the loss of activity was caused by the addition of the recognition sequence or the 6xHis tag, or both. Thus, we sought to develop more constructs in order to (a) identify at least one construct that retained WT levels of activity and (b) better understand which sequence modification contributed more significantly to the loss of function observed for yARF-6xHis-CaM.

As summarized below, we selected a second recognition sequence, derived from the N-terminal region of CaN-B (MGNEASYPL), to enable labeling of CaM by NMT. We also explored the use of flexible linkers, postulating that the placement of additional

features upstream of CaM might have a smaller effect on CaM activity if an intervening spacer were present. A number of CaM fusion proteins have been reported, including multiple GFP-CaM fusions.[7–15] In most reports, the identity of the linker was not provided or was simply incidental to the cloning scheme, with minimal quantitation of the impact of the linker on CaM activity. However, one report described an active GFP-CaM fusion in which addition of a linker (SRLIGSA) and GFP to CaM was found "not to significantly affect the functional properties of the CaM molecule."[9] Thus, we also prepared constructs possessing this linker in addition to an NMT recognition sequence. A full summary of constructs is presented in Table III-1.

Table III-1. Summary of engineered CaM constructs developed for N-terminal protein labeling studies. The yARF and hCaNB recognition sequences are derived from known NMT substrates. The 6xHis tag was included for affinity purification and immunodetection purposes. The linker was previously described.[9] Estimated yields are based on actual yields from 100 mL cultures.

Construct Name	Amino Acid Sequence Preceding CaM	Estimated Pure Yield for 1 L Culture (mg)
yARF–CaM	MGLFASK–	2
yARF-Linker–CaM	MGLFASK-SRLIGSA–	4
yARF-6xHis–CaM	MGLFASK-HHHHHH–	35
hCaNB–CaM	MGNEASYPL–	62
hCaNB-Linker–CaM	MGNEASYPL-SRLIGSA–	45

RESULTS AND DISCUSSION

Expression and Purification of CaN

We followed literature protocols for expression and purification of human CaN from an *E. coli* co-expression system.[3] In addition to growing cultures in the presence of myristic acid, we also expressed CaN in the presence of 12-ADA. Identical expression and purification results were obtained for both. Yields of 2–3 mg pure protein per liter of bacterial culture have been reported; we obtained similar yields of pure Myr-CaN and pure 12-ADA-CaN.

Cloning, Expression, and Purification of Wild-Type and Engineered CaM Constructs

To prepare plasmids that encode the engineered CaM proteins listed in Table III-1, we followed different protocols than those described in Chapter II for cloning yARF-GFP and Fyn-GFP. Using a modified site-directed mutagenesis approach, termed "two-step PCR,"[16] we encoded the desired sequences directly into primers, with a plasmid that encodes *Drosophila melanogaster* CaM serving as the template; these steps are described in detail in the Experimental Section of this chapter. This approach was considerably simpler and more efficient than the cloning strategy used to construct yARF-GFP and Fyn-GFP.

After all five constructs had been prepared, the final plasmids were transformed into *E. coli* competent cells already harboring a plasmid encoding one of the two isoforms of human NMT. Following the co-expression protocol outlined in Chapter II, we grew cultures of all five engineered CaM constructs in the presence of 12-ADA and

grew a control culture of WT CaM. We then used phenyl sepharose resin to purify the proteins from lysate.

Phenyl sepharose purification relies on a hydrophobic interaction between CaM and the sepharose resin.[17] When CaM is in its Ca^{2+}-bound form, a hydrophobic patch on the protein is exposed, and it binds the resin. At this point, wash buffers containing high concentrations of salt and Ca^{2+} remove contaminants while CaM remains bound to the column. In contrast, elution buffers contain Ca^{2+} chelators, such as EGTA, which cause CaM to give up its Ca^{2+} ions and undergo a conformational change that conceals its hydrophobic patch. CaM no longer interacts with the resin and elutes off the column. (Purification protocols are presented in more detail in the Experimental Section.)

All proteins were obtained in a very pure form after phenyl sepharose purification, as evidenced by SDS-PAGE analysis (Figure III-2). The amount of pure protein yielded by each 100 mL culture was used to estimate the per-liter yield for each protein, shown in Table III-1. Unexpectedly, the yields for yARF-CaM and yARF-Linker-CaM were consistently and significantly lower than those measured for WT CaM and the other engineered constructs. Fortunately, purification of the 12-ADA-labeled engineered constructs (Figure III-2, B-F) appeared to be unaffected by the presence of the hydrophobic 12-ADA tag when compared to the purification results for WT CaM (Figure III-2A).

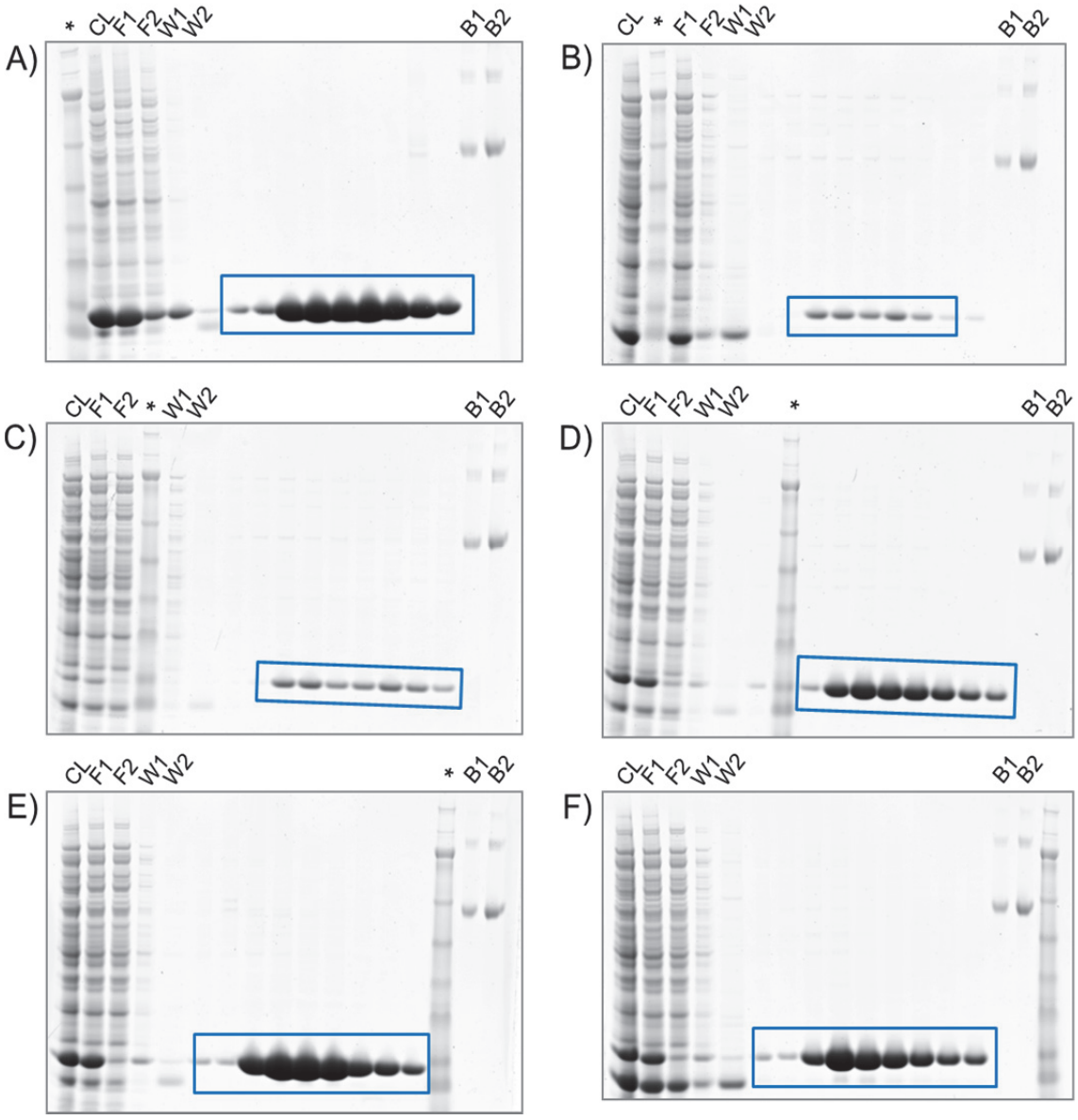

Figure III-2. SDS-PAGE analysis of phenyl sepharose purification fractions for each CaM construct. Pure protein is outlined with a blue box on each gel image: WT CaM (A); yARF-CaM (B); yARF-Linker-CaM (C); yARF-6xHis-CaM (D); hCaNB-CaM (E); hCaNB-Linker-CaM (F). All constructs except WT CaM were expressed in the presence of 12-ADA for N-terminal labeling by NMT. * = MW marker; CL = Clarified Lysate; F = Flow-Through; W = Wash. B1 = 0.05 mg/mL BSA; B2 = 0.1 mg/mL BSA.

Intact LC-MS Analysis of Protein Samples

After purifying 12-ADA-CaN, WT CaM, and 12-ADA-labeled engineered CaM constructs, we analyzed all seven proteins via intact LC-MS. As with yARF-GFP and Fyn-GFP, we observed near-quantitative labeling of all proteins displaying an NMT recognition sequence. No myristoylated protein species were detected for any samples. Across multiple expressions and purifications, yARF-CaM was the only protein for which greater than 10% unlabeled species was regularly observed; it is possible that this result is somehow correlated to the very low expression yields for this particular construct.

Table III-2. Intact LC-MS results for WT CaM and 12-ADA-labeled CaN and CaM constructs. All expected masses account for removal of the initial Met, excluding the WT CaM mass. "+12-ADA (red.)" entries correspond to labeled proteins on which the azide group was reduced to an amine. "% Labeled" = sum of the relative abundances of both 12-ADA-labeled species observed for each protein.

Protein	Expected Mass (Da)	Observed Mass (Da)	Relative Abundance	% Labeled
Human CaN, B subunit	19,168.72	N/D	N/A	> 98 %
+12-ADA	19,392.03	19,392.12	0.59	
+12-ADA (red.)	*19,366.03*	*19,363.70*	*0.41*	
WT CaM	16,679.80	16,677.38	1.00	N/A
yARF-CaM	17,283.53	17,281.28	0.12	88%
+12-ADA	17,506.84	17,504.78	0.75	
+12-ADA (red.)	*17,480.84*	*17,478.84*	*0.13*	
yARF-Linker-CaM	17,968.34	N/D	N/A	> 98 %
+12-ADA	18,191.65	18,188.88	0.75	
+12-ADA (red.)	*18,165.65*	*18,165.27*	*0.25*	
yARF-6xHis-CaM	18,106.30	N/D	N/A	> 98 %
+12-ADA	18,329.68	18,327.36	0.72	
+12-ADA (red.)	*18,303.68*	*18,302.44*	*0.28*	
hCaNB-CaM	17,511.71	N/D	N/A	> 98 %
+12-ADA	17,735.02	17,731.59	0.45	
+12-ADA (red.)	*17,709.02*	*17,706.47*	*0.55*	
hCaNB-Linker-CaM	18,196.52	18,193.50	0.07	93 %
+12-ADA	18,419.83	18,416.77	0.48	
+12-ADA (red.)	*18,393.83*	*18,391.58*	*0.45*	

An interesting pattern in the intact LC-MS results for the 12-ADA-labeled CaN and CaM constructs is the abundance of the reduced 12-ADA-labeled species across samples. We investigated the cause of the azide reduction, examining the steps in our experimental protocol that could be responsible. We wondered if the reduction was caused by the presence of DTT in the purification buffers, but the use of buffers lacking DTT did not decrease the extent of azide reduction (data not shown). We also hypothesized that 12-ADA might be reduced in the cell or growth media during the

expression itself. Thus, we conducted a time-course study with hCaNB-CaM in which 12-ADA was added to the expression culture 2 hr or 1 hr prior to inducing protein expression, or at the time of induction. We found that there was no time-dependent trend in the extent of 12-ADA reduction (Table III-3), indicating that reduction was unlikely to be occurring in the expression flask. In related work, a sample of pure 12-ADA (in which the azide group was confirmed to be intact) was analyzed on the same instrument used for intact LC-MS analysis of proteins. The major species detected was the reduced form of 12-ADA (data not shown), underscoring the notion that azide reduction most likely occurred during the actual LC-MS run.

Table III-3. Intact LC-MS results for hCaNB-CaM samples purified from expression cultures exposed to 12-ADA for different lengths of time. 12-ADA was added 2 hr or 1 hr prior to inducing protein expression, or at the time of induction (0 hr). No unlabeled hCaNB-CaM was detected in any sample, and no trend was observed for the extent of reduction of the azide moiety with respect to time. N/D = Not Detected. N/A = Not Applicable.

Time Point	Protein Species	Expected Mass (Da)	Observed Mass (Da)	Relative Abundance	% Labeled	% Reduced
2 hr	hCaNB-CaM +12-ADA *+12-ADA (red.)*	17,511.71 17,735.02 *17,709.02*	N/D 17,732.40 *17,706.87*	N/A 0.64 *0.36*	> 98 %	36%
1 hr	hCaNB-CaM +12-ADA *+12-ADA (red.)*	17,511.71 17,735.02 *17,709.02*	N/D 17,732.41 *17,706.90*	N/A 0.59 *0.41*	> 98 %	41%
0 hr	hCaNB-CaM +12-ADA *+12-ADA (red.)*	17,511.71 17,735.02 *17,709.02*	N/D 17,732.68 *17,707.13*	N/A 0.61 *0.39*	> 98 %	39%

Evaluation of CaN and Engineered CaM Constructs via Phosphatase Activity Assays

Next, we investigated the potential impact of protein engineering and labeling on the activity of our various constructs. To address this issue, we utilized a phosphatase activity assay that tests the ability of CaN to dephosphorylate a phosphopeptide substrate derived from one of its natural substrate proteins. The resultant free phosphate reacts colorimetrically with a malachite green reagent, producing a change in absorption that may be measured on a standard plate reader.[18,19] Dephosphorylation depends on proper functioning of CaN, which in turn must be bound and activated by a functional form of CaM. Moreover, both CaN and CaM are fully active only in their Ca^{2+}-bound form, a fact that is important for the assays described here and especially pertinent for the assays described in the next section.

For all of the assay results depicted in Figure III-3, the concentration of CaN was held constant, while the concentration of CaM was varied over roughly four orders of magnitude. Ca^{2+} was also present at a saturating level. After CaN, CaM, and Ca^{2+} were equilibrated, the phosphopeptide substrate was added to the solution to initiate the enzymatic reaction; the reaction was quenched after 10 minutes via addition of malachite green.

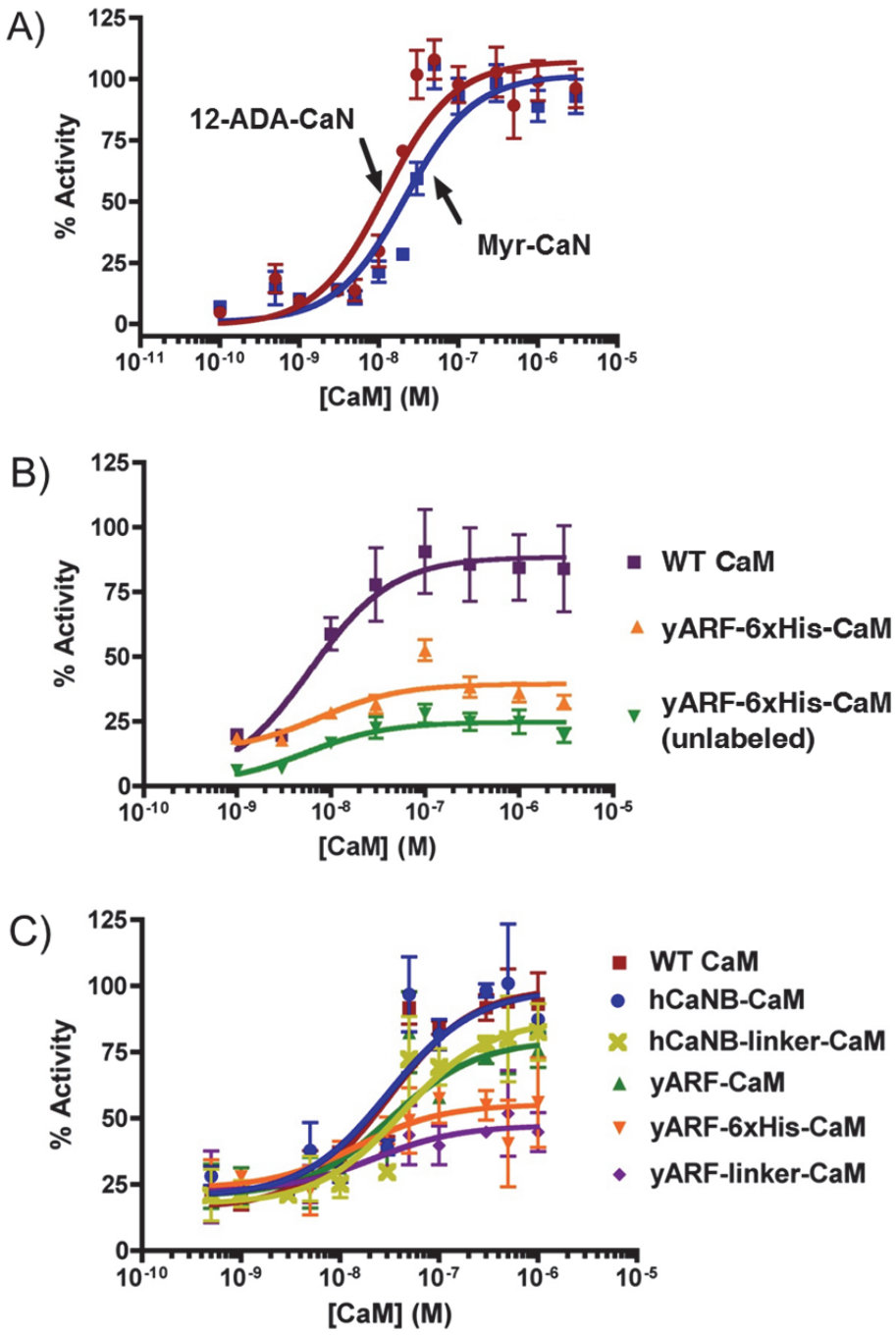

Figure III-3. Free phosphate generated upon incubation of CaN, CaM, and Ca^{2+} with RII phosphopeptide was measured in a standard Biomol Green (malachite green) phosphatase activity assay. (A) Myr-CaN or 12-ADA-CaN was incubated with saturating Ca^{2+} and varying concentrations of WT CaM. (B) CaN was incubated with saturating Ca^{2+} and varying concentrations of WT CaM, 12-ADA-labeled yARF-6xHis-CaM, or unlabeled yARF-6xHis CaM. Results in (A) and (B)

indicate that 12-ADA has little effect on CaN or CaM activity. (C) CaN was incubated with saturating Ca^{2+} and varying concentrations of WT CaM or a 12-ADA-labeled engineered CaM protein. For (A), results are presented as % activity of Myr-CaN. For (B) and (C), results are presented as % activity of WT CaM. For all graphs, $n \geq 4$.

The first graph above indicates that myristoylated CaN (Myr-CaN) and 12-ADA-CaN behave identically (Figure III-3A); we did not expect there to be much difference between these protein species because CaN is naturally myristoylated, and the azide moiety is largely inert. For our initial studies with CaM, we examined only yARF-6xHis-CaM (Figure III-3B). We found that addition of the yARF recognition sequence and the 6xHis tag resulted in a four-fold loss of activity relative to WT CaM, though the 12-ADA label did not appear to impact CaM activity. These data motivated us to prepare more engineered CaM constructs for NMT labeling, as described earlier.

After expressing and purifying the other members of the family of engineered CaM constructs, we tested them in the same phosphatase activity assay and were pleased to find that one construct, hCaNB-CaM, was as active as WT CaM (Figure III-3C). The ability to functionalize a CaM construct in a site-specific manner without an accompanying loss of activity should enable researchers to study CaM in a variety of settings, such as in single-molecule fluorescence experiments or on protein microarrays. Considering the ubiquity of CaM in eukaryotes, and given the large number of proteins that CaM binds and activates, the hCaNB-CaM construct has the potential to be useful for researchers in a number of fields.

Finally, in analyzing the data presented in Figure III-C, we were also able to answer a question posed near the beginning of this chapter: is the yARF sequence or the

6xHis tag responsible for the diminished activity of yARF-6xHis-CaM? The yARF-CaM construct, which lacks a linker or affinity tag, is 25% less active than WT CaM. Addition of the linker sequence or a 6xHis tag further decreases the activity of the corresponding constructs relative to the yARF-CaM and hCaNB-CaM parent constructs. Thus, it seems that both the yARF sequence and the 6xHis tag contribute to the poor activity of yARF-6xHis-CaM. With a different recognition sequence and no linker or 6xHis tag, and with wild-type levels of activity, hCaNB-CaM is clearly the construct of choice for future studies.

Calcium-Binding Behavior of Engineered CaM Constructs

To obtain a better understanding of our engineered CaM constructs, we investigated their Ca^{2+}-binding behavior with two different methods: a conventional electrophoretic mobility assay ("gel shift assay") described in the literature to probe other CaM mutants,[9,20] and the phosphatase activity assay described in the previous section.

The electrophoretic mobility assay exploits the change in the apparent molecular weight of CaM during SDS-PAGE depending on the buffer environment. As noted above, CaM undergoes a significant conformational change upon binding Ca^{2+}, exposing a hydrophobic patch on the protein. This structural change results in CaM running to a lower molecular weight in the presence of saturating levels of Ca^{2+}. In contrast, when CaM is in the presence of Ca^{2+} chelators, it runs to a higher apparent molecular weight. By utilizing SDS-PAGE buffers containing high concentrations of Ca^{2+} or EDTA, we found that our engineered and 12-ADA-labeled CaM constructs underwent a shift similar

to that of WT CaM: all six proteins appear to bind Ca^{2+} similarly at saturating levels of Ca^{2+} (Figure III-4A).

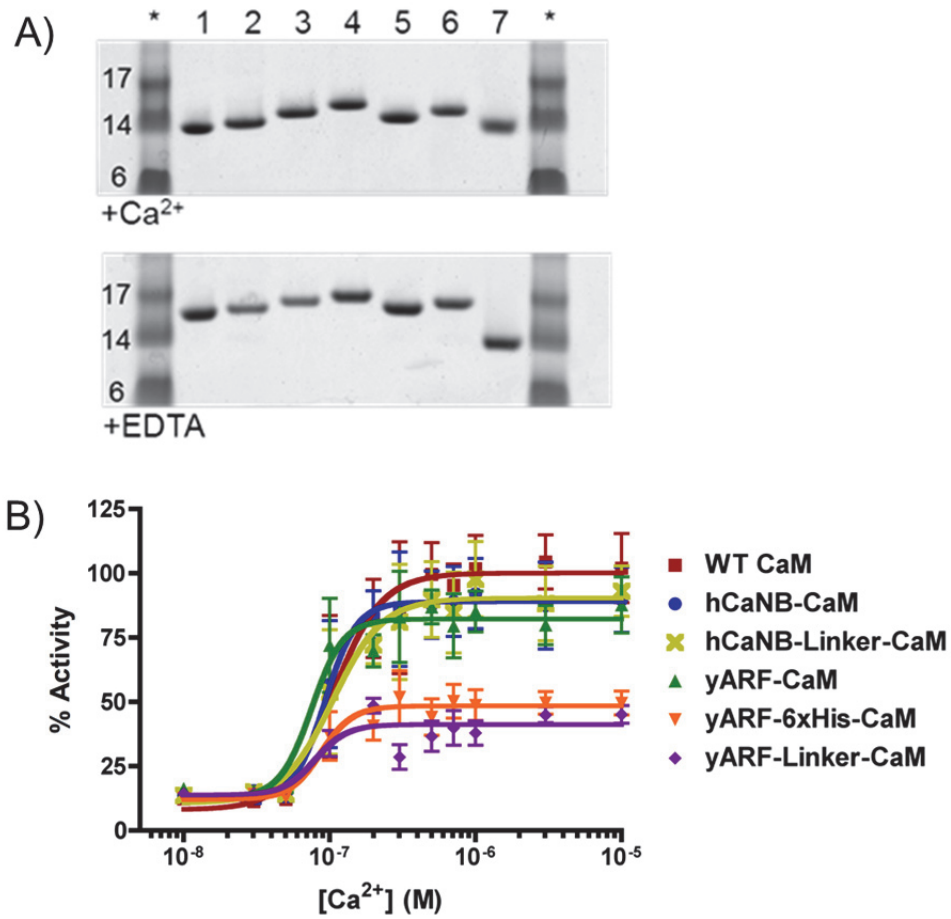

Figure III-4. (A) WT CaM and 12-ADA-labeled engineered CaM proteins were examined in an electrophoretic mobility ("gel shift") assay. SDS-PAGE buffers contained either Ca^{2+} (top) or EDTA (bottom). Coomassie staining revealed a Ca^{2+}-dependent shift in apparent mass for WT CaM (1), as well as for all 12-ADA-labeled engineered CaM proteins: yARF-CaM (2), yARF-Linker-CaM (3), yARF-6xHis-CaM (4), hCaNB-CaM (5), and hCaNB-Linker-CaM (6). Lysozyme (7) served as a negative control for Ca^{2+}-dependent mobility. Protein marker lanes are denoted by *. (B) CaN was incubated with saturating CaM (WT CaM or a 12-ADA-labeled engineered CaM protein) and varying concentrations of Ca^{2+}; then, free phosphate was detected in a standard Biomol Green (malachite green) activity assay. Results are presented as % activity of WT CaM; $n \geq 4$.

The phosphatase activity assay provided a more quantitative measure of the Ca^{2+}-binding behavior of our family of CaM constructs. The assay was carried out exactly as previously described, but instead of varying the concentration of CaM, we used a saturating level of CaM and varied the concentration of Ca^{2+} (Figure III-4B). Again, hCaNB-CaM was found to be the most active construct relative to WT CaM, with the other proteins exhibiting diminished activity in roughly the same order as was observed in the [CaM]-dependent phosphatase assay (Figure III-3C). All of the K_D values measured in our activity assay studies are summarized in Table III-4.

Table III-4. Binding constants for activity assay graphs (Figures III-3A, III-3C, and III-4B). Values are reported as ± standard error. ND = Not Determined.

Protein	[CaM]-Dependent Activity Assay: K_D (nM)	[Ca^{2+}]-Dependent Activity Assay: K_D (nM)
Myr-CaN	21 ± 12	-
12-ADA-CaN	12 ± 12	-
WT CaM	31 ± 14	107 ± 12
hCaNB-CaM	31 ± 14	93 ± 12
hCaNB-Linker-CaM	43 ± 16	105 ± 12
yARF-CaM	33 ± 17	75 ± 12
yARF-6xHis-CaM	ND	87 ± 12
yARF-Linker-CaM	ND	79 ± 13

Fluorescence Gel Analysis of Lysate Samples

Before proceeding to surface capture experiments with 12-ADA-CaN and 12-ADA-hCaNB-CaM, we wanted to confirm that NMT is selective toward our constructs in *E. coli*. In order to couple our proteins to microarrays directly from lysate,

it was important to establish that proteins other than our substrates were not labeled by NMT. Utilizing experimental protocols optimized for the GFP/NMT model system, we examined clarified lysate samples of CaN and the engineered CaM constructs after *in vivo* labeling with 12-ADA. For CaM, we focused on the two most active constructs: hCaNB-CaM and hCaNB-Linker-CaM. (Similar results were obtained for the remainder of the constructs, though yARF-CaM and yARF-Linker-CaM were difficult to detect in this experiment due to their low expression levels.) The gel images presented in Figure III-5 confirm that NMT is indeed selective toward CaN and the engineered CaM constructs in bacteria: fluorescent bands appear only at the molecular weight values for CaN-B and the engineered CaM proteins.

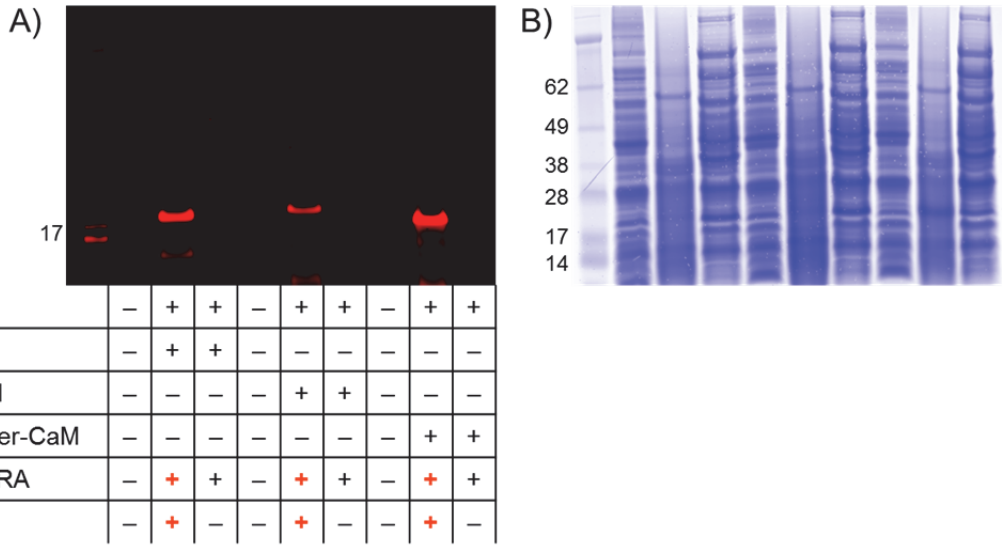

Figure III-5. SDS-PAGE analysis of lysate samples of CaN, hCaNB-CaM, and hCaNB-Linker-CaM co-expressed with NMT in the presence of 12-ADA. Lysate samples were treated with alkyne-TAMRA for detection of azide-labeled protein. The gel was imaged for TAMRA (A) and stained with Coomassie colloidal blue (B). Comparison of both gel images indicates selective 12-ADA labeling of each natural or engineered substrate protein. Similar results were obtained for other engineered CaM constructs.

CONCLUSION

The work presented in this chapter significantly expands the scope of the NMT-mediated protein labeling system developed in Chapter II. In moving beyond the test protein, GFP, we demonstrated the versatility and power of the system with proteins of real biomedical interest, calcineurin (CaN) and calmodulin (CaM). A natural substrate of NMT, CaN was shown to be equally active in its myristoylated and 12-ADA-labeled forms. Engineering of CaM to display different NMT recognition sequences also resulted in robust protein labeling with 12-ADA, as measured by intact LC-MS. Phosphatase activity assays investigating the behavior of the engineered CaM constructs showed that hCaNB-CaM was as active as WT CaM in both CaM-dependent and Ca^{2+}-dependent assays. Finally, treatment of lysate samples with an azide-reactive dye confirmed that only the CaN and CaM-based substrates were labeled with 12-ADA by NMT, enabling the preparation of protein microarrays from lysate, as described in the next chapter.

EXPERIMENTAL SECTION

Materials

Cloning. All oligonucleotide primers were ordered from IDT. The pET-15b plasmid encoding *Drosophila melanogaster* wild-type calmodulin was a gift from Professor Steven Mayo's lab at Caltech. The QuikChange site-directed mutagenesis kit was used as is from Stratagene/Agilent. Polymerase chain reaction (PCR) experiments were carried out in a BioRad DNA Engine Peltier Thermal Cycler using PfuTurbo DNA Polymerase (Stratagene/Agilent). All restriction enzymes, restriction enzyme buffers,

bovine serum albumin (BSA), and ligase were purchased from New England BioLabs (NEB). NEB DNA Ladders (100 bp and 1 kbp "Quick-Load") were used as markers for all DNA agarose gels, which were visualized with the addition of Plus One ethidium bromide solution from Amersham Biosciences on a UVP UV Transilluminator. Zymo Agarose-Dissolving Buffer (ADB) and Zymo Spin II columns, with their associated buffers, were used to purify DNA out of agarose gels. All DNA acquisition from cells was completed using the Qiagen Spin Miniprep Kit and columns. All sequencing requests were fulfilled by Laragen.

Protein expression. Plasmids encoding hNMT1 or hNMT2 and methionine-aminopeptidase (Met-AP) were a gift from the laboratory of Professor Richard Kahn at Emory University (Atlanta, GA).[21] The plasmid encoding human CaN^3 was purchased from Addgene. *E. coli* BL21(DE3) chemically competent cells were prepared using the standard Zymo method (Stratagene) and were transformed with either the hNMT1 plasmid or hNMT2 plasmid. LB medium was composed of 10 g tryptone (casein hydrolysate), 5 g yeast extract, and 10 g NaCl per liter. Media were autoclaved before use. Kanamycin (Kan) was used at a working concentration of 35 μg/mL, and ampicillin (Amp) was used at a working concentration of 200 μg/mL. Myristic acid was purchased from Fluka. All optical density (OD) values were measured at 600 nm on a Cary UV-Vis spectrophotometer. All SDS-PAGE gels described in this chapter were NuPAGE Novex 4%–12% Bis-Tris pre-cast gels (Invitrogen). SeeBlue Plus2 Pre-Stained Protein Marker from Invitrogen served as the molecular weight ladder. Gels were stained with Coomassie colloidal blue from Invitrogen.

Protein purification. CaN was purified with Talon cobalt affinity resin (Clontech) and calmodulin-sepharose 4B resin (GE Healthcare); Nickel-NTA resin from Qiagen could be used in place of Talon resin, if desired. All lysis, wash, and elution buffers were prepared exactly as reported.[3] Lysozyme was purchased from Aldrich.

CaM and engineered CaM constructs were purified using phenyl sepharose resin from GE Healthcare. (The yARF-6xHis-CaM protein was also purified using Qiagen Ni-NTA resin, in a manner identical to that described in Chapter II for yARF-GFP and Fyn-

GFP.) For CaM purification, the Lysis Buffer was 50 mM Tris (pH 7.5), 100 mM KCl, 1 mM EDTA, 1 mM EGTA, 1 mM DTT, 1 mg/mL lysozyme, and 0.5 mM PMSF; Wash Buffer 1 was 50 mM Tris (pH 7.5) and 1 mM $CaCl_2$; Wash Buffer 2 was 50 mM Tris (pH 7.5), 1 mM $CaCl_2$, and 500 mM NaCl; and Elution Buffer was 50 mM Tris (pH 7.5) and 1.5 mM EGTA. Lysozyme was purchased from Aldrich.

Mass spectrometry analysis. The Pierce BCA Assay Kit was used to measure protein concentration in pure protein fractions prior to MS analysis. Millipore Microcon Centrifugal Devices were used to concentrate and buffer-exchange whole-protein samples for intact LC-MS analysis, which was carried out on an Agilent 1100 MSD quadrupole ESI-MS.

Phosphatase activity assays. Human recombinant WT CaM, human recombinant WT myristoylated CaN, and Biomol Green (malachite green) reagent were purchased from Enzo Life Sciences. The phosphorylated CaN-specific substrate peptide (pRII peptide) was purchased from GenScript. All other reagents were reagent grade and purchased from Sigma-Aldrich. Assay Buffer was composed of 50 mM Tris (pH 7.5), 100 mM NaCl, 6 mM $MgCl_2$, and 0.5 mM DTT.

Electrophoretic mobility assay. Buffers for the electrophoretic mobility assay was prepared as described.[9,20] In summary, 5x Loading Buffer was 0.225 M Tris (pH 6.8) containing 50% glycerol, 5% SDS, and 0.05% bromophenol blue. To 1 mL of the Loading Buffer, either 2 μL of 1 M $CaCl_2$ was added for a final concentration of 2 mM $CaCl_2$ (for the $+Ca^{2+}$ gel), or 6 μL of 0.5 M EDTA was added for a final concentration of 3 mM EDTA (for the +EDTA gel). Running Buffer was MES running buffer (Boston BioProducts); to 1 L of the commercially available running buffer, which already contained 1 mM EDTA, either 3 mL of 1 M $CaCl_2$ was added to achieve a final effective concentration of 2 mM $CaCl_2$ (for the $+Ca^{2+}$ gel), or 4 mL of 0.5 M EDTA was added to achieve a final concentration of 3 mM EDTA (for the +EDTA gel). SDS-PAGE gels were NuPAGE Novex 4%–12% Bis-Tris pre-cast gels, and SeeBlue Plus2 Pre-Stained Protein Marker served as the molecular weight ladder (both from Invitrogen). Gels were stained with Coomassie colloidal blue, also from Invitrogen.

Fluorescence detection. Lysate samples were treated with the reagents and according to the protocols of the Click-IT Tetramethylrhodamine (TAMRA) Protein Analysis Detection Kit from Invitrogen. After reaction and precipitation, protein samples were run on Invitrogen NuPAGE Novex 4%–12% Bis-Tris pre-cast gels and imaged on a GE Typhoon laser scanner. Gels were stained with Coomassie colloidal blue from Invitrogen.

Methods

Cloning. The template plasmid for all engineered CaM constructs was pET-15b encoding *Drosophila melanogaster* wild-type CaM. Primers were designed to encode the amino acid sequences corresponding to the constructs outlined in Table III-1: the yARF recognition sequence (MGLFASK, from ATG GGT CTG TTC GCG TCT AAA), the hCaNB recognition sequence (MGNEASYPL, from ATG GGT AAC GAA GCG TCT TAC CCG CTG), a 6xHis tag, and/or the linker sequence (SRLIGSA, from TCT CGT CTG ATC GGT TCT GCT) at the 5′ end of the gene. The QuikChange site-directed mutagenesis kit was used in conjunction with published protocols for the "two-step PCR" method; this approach circumvents "the tendency of the perfectly complementary mutagenic primers to dimerize with each other, rather than anneal to the target sequence [in the parent plasmid]," and thus enables the addition of long insertions.[16] Briefly, for each construct, two single-primer PCR reactions were carried out to produce "hybrid" plasmids, comprised of one original (wild-type CaM) strand and one new (mutant) strand possessing the given sequence(s). Then, in a second PCR step, the two reactions from the first step were combined and more polymerase was added to the reaction mixture. After digestion with DpnI, the mixture was transformed into XL1-Blue competent cells and plated. Colonies were selected for inoculation of cultures from which DNA was isolated and submitted for sequencing. Each final construct was transformed into competent cells already harboring an NMT plasmid for co-expression experiments.

Protein expression. Overnight cultures were inoculated in LB supplemented with Kan and Amp and grown in an incubator-shaker (37°C, 250 rpm). The following

day, overnight cultures were diluted 1:50 into fresh LB supplemented with Kan and Amp for expression cultures, which ranged in volume from 5 mL to 100 mL. Cultures were grown in an incubator-shaker (37°C, 250 rpm), and protein expression was induced with IPTG (1 mM, from 1 M stock in water) when the OD_{600} value was between 0.8 and 1.1. Pre-induction samples (1 mL) were collected as needed. Myristic acid or the azide fatty acid 12-ADA (500 μM, from 500 mM stock in DMSO) was also added at the time of induction. After 3–4 hr of protein expression, cells were harvested via centrifugation (10 min x 10,000 *g*) and the final OD_{600} value was measured. Cell pellets were lysed according to the following formula, regardless of which lysis buffer was used: 50 μL lysis buffer per mL culture per OD_{600} unit. Crude lysates were centrifuged once more, and the supernatant (clarified lysate) was saved for further experiments.

Protein purification. Published protocols were followed with minor modifications for purification of CaN and CaM constructs.

For CaN, a three-step protocol is described to purify the enzyme from bacterial lysate.[3] Briefly, harvested cells were lysed using a probe sonicator and lysozyme (1 mg/mL). The three steps are an ammonium sulfate (high-salt) precipitation, a Talon cobalt affinity resin purification step, and CaM–sepharose chromatography. All buffers were prepared and used exactly as reported in the literature to yield pure human CaN. All purification fractions were analyzed via SDS-PAGE for detection of pure protein.

For CaM, a one-step phenyl sepharose purification is reported to isolate the protein from bacterial lysate.[17,22] When CaM is in its Ca^{2+}-bound form, a hydrophobic patch on the protein is exposed, and it binds the phenyl sepharose resin; CaM elutes from the resin in the presence of buffers containing Ca^{2+} chelators, which cause CaM to undergo a conformational change that hides its hydrophobic patch. Briefly, harvested cells were lysed in Lysis Buffer using a probe sonicator and lysozyme (1 mg/mL). Clarified lysate was incubated with phenyl sepharose at 4°C for 30 min to ensure binding between CaM and the resin. The slurry was poured into a column and washed alternately with Wash Buffers 1 and 2. Then elution fractions were collected upon addition of Elution Buffer to the column. All purification fractions were analyzed via SDS-PAGE for detection of pure protein.

Mass spectrometry analysis. For intact LC-MS experiments, solutions of pure protein were concentrated using Microcon columns (MWCO = 30 kDa) and buffer-exchanged into a 0.1% TFA (trifluoroacetic acid) solution. A final solution of 100 pmol protein in 100 μL was run on the MSD instrument.

Phosphatase activity assays: [CaM]-dependent assays. The Ca^{2+}/CaM-activated phosphatase activity of CaN was determined using the malachite green assay, a colorimetric technique employed for quantitatively measuring the amount of inorganic phosphate released by dephosphorylation of a CaN-specific peptide substrate, pRII. This assay takes advantage of the green color produced by the complex formed between malachite green, molybdate, and free phosphate (PO_4).[18,19]

Briefly, varying concentrations of WT CaM were incubated with saturating Ca^{2+} (10 μM $CaCl_2$) and 10 nM Myr-CaN or 12-ADA-CaN in Assay Buffer for 10 min at 37°C. To initiate the reaction, phosphorylated RII peptide substrate was added at a final concentration of 0.5 mM in 50 μL and allowed to react for 10 min. A standard curve of inorganic phosphate (PO_4) in Assay Buffer was made on each day of experiments. A quantity of 50 μL of Biomol Green reagent (containing malachite green and molybdate) was added to the standard curve and experimental samples to terminate the reaction, and color was allowed to develop for 30 min. The absorbance of all samples was measured at 620 nm on a Tecan 96-well plate reader. The absorbance values of the standard curve were plotted against the (known) concentrations of the PO_4 standards and fit to a second-order polynomial, from which the amount of CaN-mediated release of PO_4 in the samples was calculated. The CaN phosphatase activity was plotted as a function of CaM concentration using Prism (GraphPad Software). The dose-response of CaN activity at varying CaM concentrations was calculated according to the sigmoidal dose response (Equation (1)):

$$Y = \min + \frac{max - min}{1 + 10^{Log(X50 - X)}} \qquad (1)$$

where X is the concentration, Y is the response, min is the lower asymptote of the curve, max is the upper asymptote of the curve, and X50 is the x-coordinate of the inflection point (x, y). X50 represents the concentration at which CaN is half-maximally activated and is directly related to the ability of CaM to bind and activate CaN.

Phosphatase activity assays: [Ca^{2+}]-dependent assays. The ability of the 12-ADA-labeled engineered CaM proteins to bind and activate CaN was measured using the malachite green assay described above in order to determine the CaM constructs' Ca^{2+}-dependent activation. Briefly, 10 nM Myr-CaN, 1 μM wild-type CaM or engineered labeled CaM, and varying concentrations of free Ca^{2+} were incubated at 37°C for 10 min. The concentration of free Ca^{2+} was tightly controlled by titration of the calcium chelator EGTA.[23] The reaction was initiated by addition of phosphorylated RII peptide substrate at a final concentration of 0.5 mM in 50 μL. The reaction was allowed to proceed for 10 min at 37°C. A standard curve of inorganic phosphate (PO_4) in Assay Buffer was made on each day of experiments. Biomol Green reagent (50 μL) was added to the standard curve and experimental samples to terminate the reaction, and color was allowed to develop for 30 min. The absorbance of all samples was measured at 620 nm on a Tecan 96-well plate reader. The absorbance values of the standard curve were plotted against known concentrations of PO_4 and fit to a second-order polynomial, from which the amount of CaN-mediated release of PO_4 in the samples was interpolated. The CaM-mediated CaN phosphatase activity as a function of Ca^{2+} concentration was plotted using Prism (GraphPad Software). The dose-response of activity of the same was calculated according to Equation (1).

Electrophoretic mobility assay. These experiments were conducted according to literature protocols.[9,20] Two different gels were run: a +Ca^{2+} gel, in which samples were exposed to an environment containing saturating levels of Ca^{2+}, and a +EDTA gel, in which samples were exposed to an environment containing excess EDTA. Samples of pure wild-type CaM, engineered CaM proteins, and lysozyme were prepared at equal concentrations, and 10 μg of each protein was loaded on a protein gel using the Loading Buffers described in the Materials section. SDS-PAGE was performed using the Running Buffers described in the Materials section. Gels were stained with Coomassie colloidal blue and imaged on the Typhoon with the 633 nm laser serving as the excitation source (no filter).

Fluorescence detection. Cells were lysed with the buffer recommended in the instructions for the Invitrogen Click-iT kit (1% SDS, 50 mM Tris-HCl, pH 8.0) according to the following formula: 50 μL lysis buffer per mL culture per OD_{600} unit. Lysate samples were reacted with alkyne-TAMRA and other kit reagents according to the protocols supplied by Invitrogen; the only modification was the use of 15 μL of alkyne-TAMRA dye solution rather than 100 μL. At the conclusion of the 25-min reaction time, samples were precipitated following the methanol-chloroform precipitation protocol described in the same kit instructions; the only modification was the completion of one extra methanol wash of the protein pellet. For SDS-PAGE analysis, protein pellets were resuspended in a denaturing buffer (8 M urea, 100 mM NaH_2PO_4, and 10 mM Tris-Cl) and loaded on a NuPAGE Novex 4%–12% Bis-Tris pre-cast gel. To detect TAMRA signal on the Typhoon, the 532 nm laser served as the excitation source (filter set: 580 BP 30). Gels were stained with Coomassie colloidal blue, then imaged again, with the 633 nm laser now serving as the excitation source (no filter).

REFERENCES

1. Squire, L. R. *et al. Fundamental Neuroscience, 2nd Ed.* (Academic Press/Elsevier Science: San Diego, CA, 2003).

2. Towler, D., Gordon, J. I., Adams, S. P. & Glaser, L. The biology and enzymology of eukaryotic protein acylation. *Annu. Rev. Biochem.* **57**, 69–99 (1988).

3. Mondragon, A. *et al.* Overexpression and purification of human calcineurin alpha from Escherichia coli and assessment of catalytic functions of residues surrounding the binuclear metal center. *Biochemistry* **36**, 4934–42 (1997).

4. Miyakawa, T. *et al.* Conditional calcineurin knockout mice exhibit multiple abnormal behaviors related to schizophrenia. *Proc. Natl. Acad. Sci. U. S. A.* **100**, 8987–92 (2003).

5. Means, A. R., Tash, J. S. & Chafouleas, J. G. Physiological implications of the presence, distribution, and regulation of calmodulin in eukaryotic cells. *Physiol. Rev.* **62**, 1–39 (1982).

6. Xia, Z. & Storm, D. R. The role of calmodulin as a signal integrator for synaptic plasticity. *Nat. Rev. Neurosci.* **6**, 267–76 (2005).

7. Mori, M. X., Imai, Y., Itsuki, K. & Inoue, R. Quantitative measurement of Ca(2+)-dependent calmodulin-target binding by Fura-2 and CFP and YFP FRET imaging in living cells. *Biochemistry* **50**, 4685–96 (2011).

8. Bal, M., Zaika, O., Martin, P. & Shapiro, M. S. Calmodulin binding to M-type K+ channels assayed by TIRF/FRET in living cells. *J. Physiol.* **586**, 2307–20 (2008).

9. Li, C. J. *et al.* Dynamic redistribution of calmodulin in HeLa cells during cell division as revealed by a GFP-calmodulin fusion protein technique. *J. Cell Sci.* **112**, 1567–77 (1999).

10. Miyawaki, A. *et al.* Fluorescent indicators for Ca(2+) based on green fluorescent proteins and calmodulin. *Nature* **388**, 882–7 (1997).

11. Griesbeck, O., Baird, G. S., Campbell, R. E., Zacharias, D. A. & Tsien, R. Y. Reducing the environmental sensitivity of yellow fluorescent protein: mechanism and applications. *J. Biol. Chem.* **276**, 29188–94 (2001).

12. Erickson, M. G., Alseikhan, B. a, Peterson, B. Z. & Yue, D. T. Preassociation of calmodulin with voltage-gated Ca(2+) channels revealed by FRET in single living cells. *Neuron* **31**, 973–85 (2001).

13. Jenikova, G., Lao, U. L., Gao, D., Mulchandani, A. & Chen, W. Elastin-calmodulin scaffold for protein microarray fabrication. *Langmuir* **23**, 2277–9 (2007).

14. Moser, M. J., Flory, M. R. & Davis, T. N. Calmodulin localizes to the spindle pole body of Schizosaccharomyces pombe and performs an essential function in chromosome segregation. *J. Cell Sci.* **110**, 1805–12 (1997).

15. Nagai, T., Sawano, A., Park, E. S. & Miyawaki, A. Circularly permuted green fluorescent proteins engineered to sense Ca(2+). *Proc. Natl. Acad. Sci. U. S. A.* **98**, 3197–202 (2001).

16. Wang, W. & Malcolm, B. A. Two-stage PCR protocol allowing introduction of multiple mutations, deletions and insertions using QuikChange site-directed mutagenesis. *Biotechniques* **26**, 680–2 (1999).

17. Gopalakrishna, R. & Anderson, W. B. Ca(2+)-induced hydrophobic site on calmodulin: application for purification of calmodulin by phenyl-sepharose affinity chromatography. *Biochem. Biophys. Res. Commun.* **104**, 830–6 (1982).

18. Martin, B., Pallen, C. J., Wang, J. H. & Graves, D. J. Use of fluorinated tyrosine phosphates to probe the substrate specificity of the low molecular weight phosphatase activity of calcineurin. *J. Biol. Chem.* **260**, 14932–7 (1985).

19. Harder, K. W. *et al.* Characterization and kinetic analysis of the intracellular domain of human protein tyrosine phosphatase beta (HPTP beta) using synthetic phosphopeptides. *Biochem. J.* **298**, 395–401 (1994).

20. Rhyner, J. A., Koller, M., Durussel-Gerber, I., Cox, J. A. & Strehler, E. E. Characterization of the human calmodulin-like protein expressed in Escherichia coli. *Biochemistry* **31**, 12826–32 (1992).

21. Van Valkenburgh, H. A. & Kahn, R. A. Coexpression of proteins with methionine aminopeptidase and/or N-myristoyltransferase in Escherichia coli to increase acylation and homogeneity of protein preparations. *Methods Enzymol.* **344**, 186–93 (2002).

22. Putkey, J. A., Slaughter, G. R. & Means, A. R. Bacterial expression and characterization of proteins derived from the chicken calmodulin cDNA and a calmodulin processed gene. *J. Biol. Chem.* **260**, 4704–12 (1985).

23. Bers, D. M. A simple method for the accurate determination of free [Ca] in Ca-EGTA solutions. *Am. J. Physiol. Cell Physiol.* **242**, C404–8 (1982).